International Journal of Pharmaceutics 639 (2023) 122982

Contents lists available at ScienceDirect

International Journal of Pharmaceutics

journal homepage: www.elsevier.com/locate/ijpharm

Cell penetrating peptides-functionalized Licochalcone-A-loaded PLGA nanoparticles for ocular inflammatory diseases: Evaluation of *in vitro* anti-proliferative effects, stabilization by freeze-drying and characterization of an in-situ forming gel

Ruth M. Galindo-Camacho [a,b,c,d], Isabel Haro [c], María J. Gómara [c], Marta Espina [b,d], Joel Fonseca [a], Carlos Martins-Gomes [e,f], Antoni Camins [g,h], Amélia M. Silva [e,f], María L. García [b,d], Eliana B. Souto [a,i,j,*]

[a] *Department of Pharmaceutical Technology, Faculty of Pharmacy, University of Porto, Rua de Jorge Viterbo Ferreira, 228, 4050-313 Porto, Portugal*
[b] *Department of Pharmacy and Pharmaceutical Technology, and Physical Chemistry, Faculty of Pharmacy and Food Sciences, University of Barcelona, 08028 Barcelona, Spain*
[c] *Unit of Synthesis and Biomedical Applications of Peptides, IQAC-CSIC, 08034 Barcelona, Spain*
[d] *Institute of Nanoscience and Nanotechnology (IN2UB), University of Barcelona, 08028 Barcelona, Spain*
[e] *Department of Biology and Environment, University of Trás-os-Montes e Alto Douro, UTAD, Quinta de Prados, P-5001-801 Vila Real, Portugal*
[f] *Centre for Research and Technology of Agro-Environmental and Biological Sciences, CITAB, UTAD, Quinta de Prados, P-5001-801 Vila Real, Portugal*
[g] *Biomedical Research Networking Centre in Neurodegenerative Diseases (CIBERNED), 28031 Madrid, Spain*
[h] *Department of Pharmacology and Therapeutic Chemistry, Faculty of Pharmacy, University of Barcelona, 08028 Barcelona, Spain*
[i] *UCIBIO – Applied Molecular Biosciences Unit, MEDTECH, Laboratory of Pharmaceutical Technology, Department of Drug Sciences, Faculty of Pharmacy, University of Porto, 4050-313 Porto, Portugal*
[j] *Associate Laboratory i4HB - Institute for Health and Bioeconomy, Faculty of Pharmacy, University of Porto, 4050-313 Porto, Portugal*

ARTICLE INFO

Keywords:
Licochalcone-A
PLGA nanoparticles
Cell penetrating peptide
Freeze-drying
In-situ forming gel
Ocular anti-inflammatory

ABSTRACT

Licochalcone-A (Lico-A) PLGA NPs functionalized with cell penetrating peptides B6 and Tet-1 are proposed for the treatment of ocular anti-inflammatory diseases. In this work, we report the *in vitro* biocompatibility of cell penetrating peptides-functionalized Lico-A-loaded PLGA NPs in Caco-2 cell lines revealing a non-cytotoxic profile, and their anti-inflammatory activity against RAW 264.7 cell lines. Given the risk of hydrolysis of the liquid suspensions, freeze-drying was carried out testing different cryoprotectants (e.g., disaccharides, alcohols, and oligosaccharide-derived sugar alcohol) to prevent particle aggregation and mitigate physical stress. As the purpose is the topical eye instillation of the nanoparticles, to reduce precorneal wash-out, increase residence time and thus Lico-A bioavailability, an in-situ forming gel based on poloxamer 407 containing Lico-A loaded PLGA nanoparticles functionalized with B6 and Tet-1 for ocular administration has been developed. Developed formulations remain in a flowing semi-liquid state under non-physiological conditions and transformed into a semi-solid state under ocular temperature conditions (35 °C), which is beneficial for ocular administration. The pH, viscosity, texture parameters and gelation temperature results met the requirements for ophthalmic formulations. The gel has characteristics of viscoelasticity, suitable mechanical and mucoadhesive performance which facilitate its uniform distribution over the conjunctiva surface. In conclusion, we anticipate the potential clinical significance of our developed product provided that a synergistic effect is achieved by combining the high anti-inflammatory activity of Lico-A delivered by PLGA NPs with B6 and Tet-1 for site-specific targeting in the eye, using an in-situ forming gel.

* Corresponding author at: Department of Pharmaceutical Technology, Faculty of Pharmacy of University of Porto, R. Jorge de Viterbo Ferreira 228, 4050-313 Porto, Portugal.
E-mail address: ebsouto@ff.up.pt (E.B. Souto).

https://doi.org/10.1016/j.ijpharm.2023.122982
Received 2 December 2022; Received in revised form 17 April 2023; Accepted 21 April 2023
Available online 26 April 2023

1. Introduction

One of the most common signs of eye disorders is ocular inflammation, which can affect both the anterior and the posterior segments of the eye (El-Haddad et al., 2021). Topical administration of anti-inflammatory drugs, namely corticosteroids, are effective in treating ocular surface and anterior segment inflammation, including pain and post-operative inflammation, seasonal allergic conjunctivitis keratitis or anterior uveitis (Mazet et al., 2020). But these drugs are associated with side effects including elevation of intraocular pressure and cataract formation (Comstock and DeCory, 2012), the reason why new therapeutic strategies to treat ocular inflammatory diseases are in the pipelines.

Special attention is being paid to herbal medicines derived from natural compounds because of their minimal or negligible side effects on normal tissues compared to synthetic compounds (Mittal and Kakkar, 2021). Licochalcone-A (Lico-A), a chalconoid (natural phenolic compound), isolated from the *Glycyrrhiza* species, shows many pharmacological activities, such as anti-cancer, anti-inflammatory, anti-viral and anti-angiogenic activities (Guo et al., 2019; Liu et al., 2021). Anti-inflammatory ocular activity of this drug was also reported (Galindo et al., 2022); however, the high partition coefficient and poor water solubility exhibited by Lico-A significantly affect its bioavailability when administered topically (Wang et al., 2022).

In the last few decades, nanoparticle-based drug delivery systems have been widely used, also for targeting drugs to ocular tissues (Yun et al., 2015). Among these, polymeric nanoparticles have been proposed as a suitable approach to improve corneal permeation of class II/IV drugs improving either their stability or solubility, or by promoting targeted-specific delivery (Wang et al., 2021). Synthetic polymers such as poly(lactic-*co*-glycolic acid) (PLGA) have been extensively employed in NPs production because they are approved by the US Food and Drug Administration (FDA) as they are biocompatible, biodegradable, and are able to maintain the physicochemical stability of many drugs (Badran et al., 2018).

During the last years, cell penetrating peptides (CPPs) have emerged as versatile tools to facilitate transport inside cells (Gessner and Neundorf, 2020). We have previously demonstrated that polymeric nanoparticles functionalized with two CPPs, Tet-1 and B6, increases cell penetration and efficient drug delivery to ocular cells (Galindo et al., 2022). However, PLGA NPs, when stored for a long time in liquid form, may gradually release the encapsulated drug into the medium as a consequence of hydrolysis (Makadia and Siegel, 2011). A promising method for effective long-term stabilization of these nanosized drug delivery systems is freeze-drying (Sylvester et al., 2018) during which water is removed from nanosuspensions (frozen) under vacuum by sublimation. In this process, the use of cryoprotectants is required to inhibit particle aggregation and mitigate physical stress (Kadowaki et al., 2022; Luo et al., 2021).

The topical delivery of drugs continues to be the most appropriate option for the treatment of ocular diseases, attributed to a greater patient's compliance as formulations are easy to apply. However, conventional ocular dosage forms such as solutions, suspensions, and ointments have disadvantages, including enhanced precorneal elimination, high variation of inter-individual responses and treatment efficiency, and may also cause blurred vision (Mohd Shahrizan et al., 2022). In addition, it is known that<5 % of the applied dose is bioavailable, i.e., able to reach intraocular tissues after corneal penetration. Most of these conventional forms are washed-out from the surface of the eye by blinking and lacrimal drainage in first 15–30 s after instillation, and also because of the presence of the corneal epithelium which is a barrier to drugs, and the clearance from the vasculature in the conjunctiva (Gause et al., 2016; Maulvi et al., 2021). To overcome these drawbacks, the development of formulations that ensure an extended corneal residence time and improved permeation of the drug product, thus increasing its bioavailability, is an interesting option. For that, in-situ forming gels are instilled in liquid form (exact and precise application) on-site where the gelling mechanism takes place induced by changes of temperature, pH and ionic strength, inherent to the administration site (ocular environment) (Bai et al., 2022).

Poloxamers, triblock copolymers formed by polyethylene oxide (PEO) and polypropylene oxide (PPO) units arranged in a PEO-PPO-PEO structure, also known as Pluronics, are non-ionic, water-soluble materials that have attracted much interest as pharmaceutical excipients (de Castro et al., 2022). These polymers have an amphiphilic character, presenting surface-active properties and are capable of interacting with hydrophobic surfaces and biological membranes (Singla et al., 2022). Pluronics form gels *in situ* in response to increased temperature; besides, as these polymers are transparent, they do not interfere with normal vision and are therefore more suitable for applications in ophthalmology (Bai et al., 2022).

This study focuses on the development and characterization of Lico-A, loaded in biodegradable polymeric PLGA NPs as a potential formulation for the topical administration onto the eye, improving their stability by freeze-dried, and by developing an *in-situ* forming gel system based on poloxamer 407.

2. Materials and methods

2.1. Materials

Lico-A was purchased from Amadis Chemical (Hangzhou, China) and the polymer PLGA 50:50 Resomer® RG 503H, 34 KD from Boehringer Ingelheim (Ingelheim, Germany). Maleimide-PEG-NH2 (5 kDa) was obtained from Jenkem (Beijing, China), Tween® 80, sucrose, D-(+)-trehalose dihydrate, sorbitol and maltitol were provided by Sigma-Aldrich (Merck KGaA, Darmstadt, Germany). Glycerol anhydrous was by AppliChem GmbH (Darmstadt, Germany). Poloxamer 407 (PF127) and Hexadecyltrimethylammonium bromide (CTAB) were obtained from Sigma-Aldrich (Chemie GmbH, Steinheim, Germany). Methocel A4M (MC) was from Colorcon GmbH (Idstein, Germany). Dulbecco's Modified Eagle's Medium (DMEM), fetal bovine serum (FBS), penicillin/streptomycin, L-glutamine, 0.05 % trypsin–EDTA were obtained from Gibco (Alfagene, Portugal). Alamar Blue® was from Invitrogen, Life-Technologies (Porto, Portugal). Caco-2. (Human colon adenocarcinoma cell line) and RAW 264.7 (mouse macrophages, Abelson murine leukemia virus-induced tumor cell line) were purchased from Cell Lines Service GmbH (CLS, Eppelheim, Germany). Acetone was purchased from Fisher Scientific (Loughborough, UK). Methanol and diethyl ether were obtained from Merck KGaA (Darmstadt, Germany). Water filtered through the Millipore® MilliQ system was used for all experiments and the other chemicals and reagents used in the study were of analytical grade.

2.2. Production and optimization of Licochalcone-A PLGA nanoparticles

Lico-A PLGA NPs were developed by the solvent displacement method and optimized in a 2^3 central composite factorial design, previously described by us (Galindo et al., 2022). Briefly, 10 mg of Lico-A and 80 mg of PLGA Resomer® RG 503H were solubilized in 5 mL of acetone. Once completely dissolved, this solution was dispersed dropwise, with moderate mechanical stirring, in 10 mL of the of the aqueous phase containing 0.4 % of Tween 80; this process was carried out at room temperature. Then, the organic solvent was evaporated from the suspension under reduced pressure using a rotary evaporator.

The physicochemical properties of Lico-A PLGA NPs, average size (Z_{av}) and polydispersity index (PI) were measured by Photon Correlation Spectroscopy (PCS), after a 1:10 dilution with MilliQ® water, using the Zetasizer Nano ZS (Malvern Instruments, Malvern, UK) at 25 °C. The surface charge of the particles was evaluated by means of zeta potential (ZP) and determined by laser-Doppler electrophoresis with the M3 PALS system in a Zetasizer Nano ZS (Malvern Instruments, Malvern, UK).

The entrapment efficiency (EE) was determined indirectly by measuring the non-entrapped drug, and the quantification of Lico-A in the aqueous phase was performed by reverse-phase high performance liquid chromatography (RP-HPLC) (Galindo et al., 2022), using equation (1):

$$EE(\%) = \frac{total\ \ amount\ \ of\ \ Lico-A - free\ \ amount\ \ of\ \ Lico-A}{total\ \ amount\ \ of\ \ Lico-A} x100 \quad (1)$$

For this study, the formulation with the most appropriate physico-chemical and EE characteristics was selected.

2.3. Synthesis of cell penetrating peptides and conjugation with PEG to the polymer and preparation of Lico-A PLGA-PEG-CPP NPs

The synthesis of B6 and Tet-1 peptides, their conjugation with PEG to the PLGA Resomer® RG 503H, and respective characterization were described in a previous work (Galindo et al., 2022). After that, PLGA-PEG-CPP NPs containing Lico-A were prepared by the optimized solvent displacement method described in section 2.2.

2.4. In vitro Cell-based assays

2.4.1. Cell maintainance and handling

In this study, two cell lines (Caco-2 and RAW 264.7) were used to evaluate, respectively, the anti-proliferative/cytotoxicity and anti-inflammatory activity of the drug Lico-A, blank NPs (PLGA NPs), and Lico-A PLGA-PEG-CPP NPs. Cells were maintained in complete culture media (Dulbecco's Modified Eagle Media (DMEM) supplemented with 10 % (v/v) fetal bovine serum (FBS), 1 mM L-glutamine and antibiotics (100 U/mL of penicillin and 100 μg/mL streptomycin)) in an incubator (5 % CO_2/95 % air; 37 °C, controlled humidity). Near-confluence, cells were treated as described in Silva *et al.* (Silva et al., 2020). Cells were seeded into 96-well microplates (5×10^4 cells/mL, 100 μL/well), maintained in incubator, and were allowed to adhere and stabilize for 48 h, for other details see (Andreani et al., 2014; Carbone et al., 2018; Severino et al., 2014).

2.4.1.1. Cell Viability/Cytotoxicity assay. Alamar Blue® assay (Andreani et al., 2014) was used to assess the cytotoxic effect of Lico-A and NPs on Caco-2 and RAW 264.7 cell lines. Stock solution of Lico-A, at 10 mM (3.38 mg/mL) was prepared in DMSO; and the final concentration of DMSO, in test solutions, was never higher than 1 %. Nanoformulations contain Lico-A at 1 mg/mL. After adherence and stabilization, cell culture media was removed and replaced with test solutions (100 μL/well), prepared by dilution of stock solution or of NPs formulation in FBS-free culture medium, to achieve the desired concentrations. Nanoformulations of Lico-A (at 1 mg/mL of formulation) were diluted to achieve concentrations of Lico-A from 0 to 100 μg/mL in test solution (or equivalent concentrations of carriers, from blank NPs). After 24 h exposure to test solutions, test solutions were removed and replaced by Alamar Blue solution (100 μL/well; at 10 % (v/v), in FBS-free culture medium). Absorbance was read, after 5 h incubation, at 570 nm and 620 nm, using a microplate reader (Multiskan EX, MTX Labsystems, USA). In each assay, controls were considered, non-treated cells as positive control and Alamar Blue solution alone as negative control. Positive control cells were subjected to the same procedures (i.e., replacing of media (with only FBS-free culture media), Alamar Blue solution exposure) at the same time-point as cells exposed to the test solutions. Results are expressed as cell viability (% of control, i.e., positive control), calculated as described by Andreani et al. (2014). Three independent assays were performed, each one in quadruplicates. The IC_{50} values were calculated as described in Silva *et al.* (Silva et al., 2019).

2.4.1.2. Anti-inflammatory activity. The anti-inflammatory activity of Lico-A and NPs was evaluated in RAW 264.7 cells, as described (Silva et al., 2021). Briefly, RAW 264.7 cells were seeded in 96-well plates ($5x10^4$ cells/mL, 100 μL/well) and, after 48 h, culture media was removed and replaced by test solutions at non-cytotoxic concentrations of Lico-A and of NPs (8 wells per condition), then cells were incubated for 4 h. After incubation, test solutions were removed and cells were exposed to FBS-free culture media (4 wells per condition) or to FBS-free culture media supplemented with lipopolysaccharide (LPS; at 1 μg/mL; 4 wells per condition), for additional 24 h. LPS activates TLR-4 receptors at RAW 264.7 cells plasmatic membrane, resulting in the production of cytokines and other inflammatory markers, as nitric oxide (NO) production and release; anti-inflammatory activity is here then measured by the reduction in NO release. After cells incubation (24 h), from each well, 50 μL of supernatant was removed and transferred to a new 96-wellplate, to which 50 μL/well of Griess reagent [0.1 % (w/v) *N*-(1-naphthyl) ethylenediamine dihydrochloride in water and 1 % (w/v) sulfanilamide in 5 % (w/v) H_3PO_4 (v/v)] was added. After 15 min incubation (room temperature, in the dark), absorbance was read at 550 nm (Multiskan EX microplate reader; MTX Labsystems, USA). Quantification of NO was made with resource to a standard curve performed with sodium nitrite ($NaNO_2$; in the range 0 to 100 μM) and results were expressed as percentage of positive control (i.e., nitrite production by cells only exposed to LPS), set to 100 %, that is 0 % of anti-inflammatory effect. At the end of the experiment, the other 50 μL of culture media were removed and 100 μL/well of Alamar Blue solution were added to assess the cell viability. Cell viability was assessed as described above for Caco-2 cells.

2.5. Freeze-drying of nanoparticles

For a preliminary screening, the excipients glycerol, maltitol, sucrose, trehalose, or sorbitol were selected and added to the blank NPs at 0.5, 1, and 3 % (w/v). 4 mL of each nanoparticle formulation were transferred to a glass vial and then frozen at −80 °C using a freezer Arctiko ULUF 125® (Arctiko, Denmark) and subjected to the freeze-drying process for 48 h at a pressure of 0.137 mBar in a Telstar Cryodos-80 freeze drier (Terrassa, Barcelona, Spain). The dried cakes obtained were stored at –20 °C. Once the most suitable cryoprotectant and its optimal percentage were selected, the samples were prepared with drug nanoparticles Lico-A PLGA NPs and functionalized with CPPs Lico-A PLGA-PEG-B6 NPs and Lico-A PLGA-PEG-Tet-1 NPs. Since the focus of this study was on obtaining a suitable preservation method with cryoprotectants, the same preservative freeze-drying cycle was used for all nanoparticle formulations.

2.6. Osmolality

The osmolality (mOsm/kg) of nanoparticles formulations and formulations prepared with cryoprotectants, were measured in an Osmometer Type 15 (Löser Messtechnik, Berlin, Germany).

2.7. Reconstitution of Freeze-dried nanoparticles

For the reconstitution of each freeze-dried nanoparticle formulation, a modification of the standardized protocol developed by Kulkarni *et al.* (Kulkarni et al., 2018) was used. Briefly, freeze-dried cakes were equilibrated to room temperature before being reconstituted. After that, to each formulation, the initial volume of MilliQ® water was added (milliliters of product before the freeze-drying). Each vial was manually swirled at 90 rpm in a circular motion. Swirling of the vial involved rotating around the circumference of a circle with a diameter of 10 cm. Swirling was paused at 2 min for 15 s to visually assess progress, taking care to keep the vial upright and stable to avoid it from tipping and any unsuspended cake residue moving to other parts of the vial. The vial was again swirled for 1 min followed by another 15 s observational pause. The next swirling period was 2 min (with 15 s pause). Finally, two more periods of 2-minute swirling and 15-second observational pause were

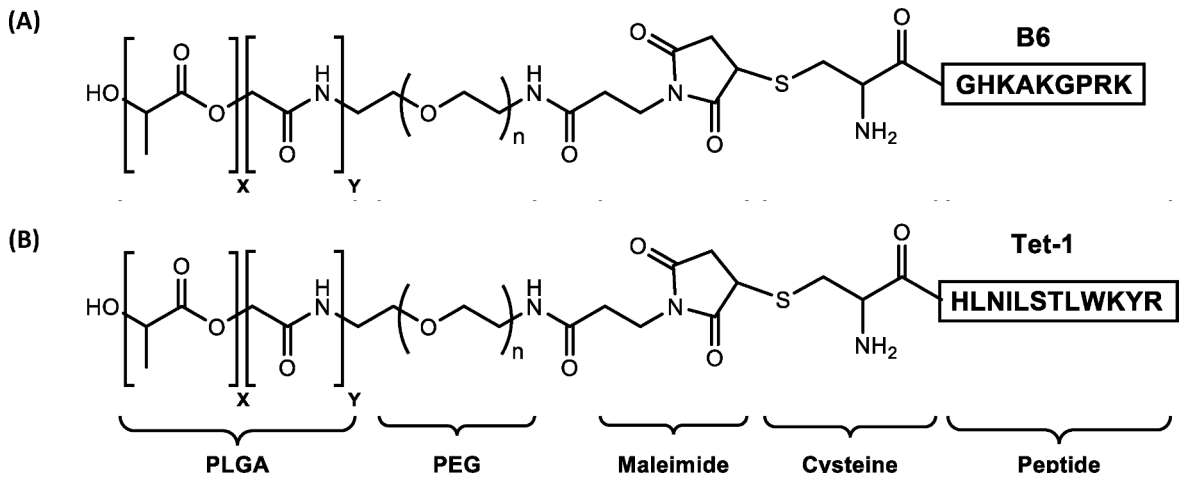

Fig. 1. **(A)** PLGA-PEG-B6 polymer, **(B)** PLGA-PEG-Tet-1 polymer.

used, and this was noted as the endpoint of reconstitution. The reconstituted solutions were visually inspected with the same criteria and the one that was totally dissolved and similar in appearance to the non-freeze-dried nanoparticles suspension control was chosen.

2.8. Differential scanning calorimetry (DSC)

DSC analysis was used to determine the physical state of Lico-A, the components of NPs formulation, and the freeze-dried functionalized nanoparticles. This study was performed in a DSC 200 F3 Maia® (NETZSCH, Germany). It consists of a double oven with two positions, one for the sample crucible to be analyzed and another for the reference crucible, which is normally empty. Samples (between 2 and 5 mg) were weighed into an aluminum crucible, which is then closed and placed in the oven. The samples are subjected to a temperature program between 10 °C and 240 °C (maximum temperature above the sample with the highest melting point), at a heating rate of 10 °C/min. The result of the analysis is translated into a thermogram, and the determination of the parameters (enthalpy, melting start temperature and melting point) is performed with the Proteus® 6.1.0B Thermal Analysis software (NETZSCH, Germany).

2.9. Preparation of in-situ forming gels

Gels were prepared dispersing 0.25 % of sodium alginate in NPs suspensions (blank NPs and Lico-A NPs) with the help of the mixer Unguator® (Gako Deutschland GmbH, Schesslitz, Germany) at 800 rpm for 3 min. One day later, MC (0–1 % w/v) and CTAB (0.2 % w/v) were added and mixed at 800 rpm for 3 min. These preparations were left to stand for a day and after that, the P407 (20 % w/v) was added and mixed to yield gels at 1000 rpm for 5 min. The *in-situ* forming gels were adjusted to pH 7.4 with NaOH and stored at 8 °C (Gonzalez-Pizarro et al., 2019).

2.10. Determination of gelation temperature of in-situ forming gels

To determine the gelation temperature, 2 mL of each formulation were prepared in glass tubes and placed in a water bath (Huber Kältemaschinenbau AG, Germany) with an initial temperature of 15 °C and then slowly heated at a rate of 1 °C/min. until detection of phase change (from solution to gel) determined by no change in the meniscus and no flow of the formed gel when tilting the vial at an angle of 180° (Mahboobian et al., 2020). The formulation with the most optimal gelation temperature near the ocular surface temperature (32–35 °C), was selected.

2.11. Characterization of in-situ forming gels

2.11.1. Texture profile analysis

This study is based on the TA-XT2i© texture analyzer from Stable Micro Systems® (Stable Micro Systems, Godalming, UK) using different probes and the Exponent software (version 6.1.12.0). For all analyzed *in-situ* Forming gels hardness, firmness, mucoadhesiveness, and spreadability at 20 °C and 35 °C were assessed. Data acquisition and analysis was performed using a computer equipped with the Texture Expert® software for all cases.

2.11.1.1. Hardness. The hardness test measures the force required to push the probe into the sample. The probe selected was P/2 2 mm Dia Cylinder Stainless with a crosshead speed of 1.5 mm s^{-1} and contact area of 3.14 mm^2. The parameter measured is the maximum force.

2.11.1.2. Firmness. The penetration method was used to determinate this parameter, which measure necessary force to produce a deformation. The probe selected was P/0.5 ½" Dia Delrin Aoac which penetrated the sample with a load cell of 5 kg, a trigger force of 0.05 N, a penetration depth of 5 mm, a velocity of 3 mm.s^{-1} and a contact area of 126.68 mm^2. The obtained results were plotted as force (N) vs distance (mm).

2.11.1.3. Mucoadhesiveness. An adhesive test was used to compare the surface stickiness of *in-situ* forming gels. The probe (A/MUC Mucoadhesion Test RIG) applied a force of 5 g on the surface of the sample at a test speed of 0.5 mm.s^{-1} holding it for 60 sec. After this time the probe was withdraw at 8 mm.s^{-1}. The maximum force necessary to overcome the attractive forces between the surface of the product and the surface of the probe was recorder as the mucoadhesiveness.

2.11.1.4. Spreadability. The spreadability test was carried out as described in a previous study (Oliveira et al., 2022). The probe was properly selected (HDP/SR Spreadability RIG) and connected to the equipment at an initial position of 25 mm after its calibration. Samples were inserted into the female cone (bottom probe) and kept in a stove at 25 °C or 35 °C ± 1 °C for 30 min before testing. For measurement, according to the method, the upper probe (male cone) penetrated the sample in the female cone at a speed of 3 mm.s^{-1} over a distance of 23 mm and then the probe returned to the starting position, providing the result. Compression and tangential forces were involved due to the conical shape of the probe.

Table 1
Physicochemical properties of the optimized formulation functionalized with CPPs.

Formulation	Z_{av} (nm) ± SD	PI ± SD	ZP (mV) ± SD	EE (%) ± SD
Lico-A PLGA-PEG-B6 NPs	114.24 ± 2.42	0.122 ± 0.012	10.49 ± 1.02	31.36 ± 0.60
Lico-A PLGA-PEG-Tet-1 NPs	128.65 ± 7.53	0.149 ± 0.016	16.02 ± 0.58	± 0.62

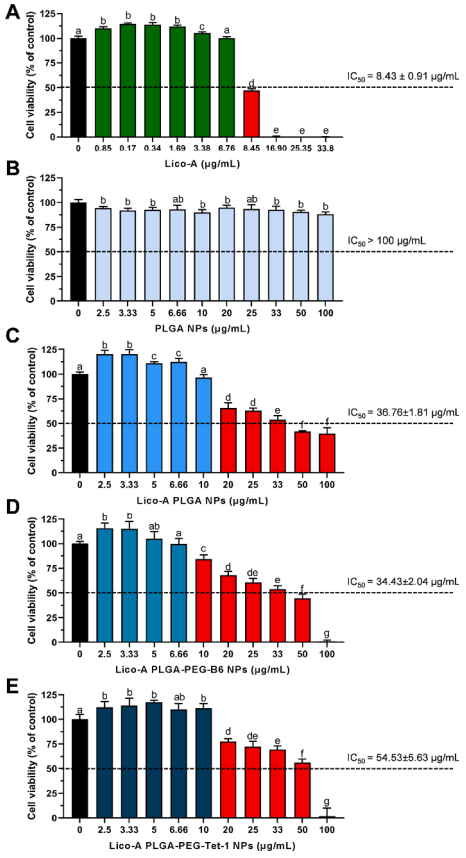

Fig. 2. Caco-2 cell viability upon exposure to Lico-A (**A**); blank NPs - PLGA NPs (**B**); Lico-A PLGA NPs (**C**); Lico-A PLGA-PEG-B6 NPs, B6 is a cell penetrating peptide (**D**); Lico-A PLGA-PEG-Tet-1 NPs, Tet1 is a cell penetrating peptide (**E**). Cells were exposed to different concentrations of Lico-A or NPs for 24 h. Cell viability was determine using AlamarBlue assay. The exposure concentrations correspond to the Lico-A concentration in formulation or equivalent for blank NPs. Results represent mean ± S.D. (n = 3 independent assays) and are expressed as percentage of control (untreated cells, positive controls). Statistically significant differences ($p < 0.05$) between the control and sample concentrations are denoted with different letters within the same sample. Concentrations that present significant decrease in cell viability are denoted as red bars. (For interpretation of the references to color in this figure legend, the reader is referred to the web version of this article.)

2.11.2. Rheological properties

Rheological properties of *in-situ* forming gels were carried out using the Kinexus Lab + Rheometer from Malvern (Malvern, Germany) equipped with the Peltier-Plate Cartridge and the CP4/40 SR4321 SS: PL61 ST S2974 SS plate geometry. A small amount of each sample was loaded onto the lower geometry of the equipment, and then torque was applied to the upper geometry, promoting shear stress on the samples. Formulations were measured at 25 °C and 35 °C ± 1 °C with a 1 mm gap between the plates. The frequency sweep was performed within the range of 0.1–10.0 Hz (final and initial frequency respectively) in the oscillation mode and the strain of 1 %, using 10 samples per decade. Data was collected using the rSpace for Kinexus Lab + software (version 1.75 Malvern Instruments).

2.12. Statistical analysis

Statistical analyses were performed by using one-way ANOVA with Tukey post hoc test. All analyzed data were presented as mean ± SD. GraphPad Prism® 9.2.0 software was used to analyze the data.

3. Results and discussion

3.1. Production and characterization of nanoparticles

After previous factorial design and analysis of the parameters affecting the NPs preparation, the optimized formulation containing 1 mg/mL of Lico-A, 8 mg/mL of PLGA, and 0.4 % of Tween80 was characterized (Galindo et al., 2022). Lico-A PLGA NPs showed a mean size of 163.81 ± 2.29 nm, with PI of 0.075 ± 0.010 and an EE of 56.26 ± 0.16 %. Although the ZP was − 24.2 ± 1.14 mV. All these characteristics are indicative that the formulation is suitable for ocular administration and has good stability (Ali and Lehmussaari, 2006).

The polymers used for obtaining NPs functionalized with the CPPs are illustrated in Fig. 1, and the results of their physicochemical properties, ZP and EE of both preparations (Lico-A PLGA-PEG-B6 NPs and Lico-A PLGA-PEG-Tet-1 NPs) are summarized in Table 1.

These values show a slightly decrease in the particle size, maybe an indicative of the polymer interactions with the positive peptide charge that compacts the NPs core. Furthermore, functionalization of nanoparticles with positively charged CPPs changed the anionic ZP to cationic. As previously described, this positive charge will promote mucoadhesion with the corneal tissues (negatively charged) due to electrostatic interactions (Mobaraki et al., 2020).

3.2. Assessment of biological effects on selected cell lines

3.2.1. Assessment of biocompatibility/cytotoxic effects of Lico-A and of NPs on Caco-2 cells

The cytotoxic effect of Lico-A and of four formulations, in the form of unloaded (PLGA-NPs) and loaded with Lico-A (Lico-A PLGA NPs, Lico-A PLGA-PEG-B6 NPs, Lico-A PLGA-PEG-Tet-1 NPs), were tested on Caco-2 cells, and results for 24 h exposure are shown in Fig. 2. As shown in Fig. 2A, Lico-A up to 6.76 µg/mL (20 µM) is not toxic as it does not reduce cell viability (cell viability ~ 100 % of control); however increasing Lico-A concentration to 8.45 µg/mL (25 µM) strongly reduces cell viability (47.2 ± 1.8 % of control) and the higher concentration reduces cell viability to ~ 0 %. This might result from the fact that Lico-A as being amphiphilic may interact with cell membranes. Concerning the cytotoxic effect of Lico-A against Caco-2 cells, we found an IC_{50} of 8.4 ± 0.9 µg/mL (Fig. 2A). This value is slightly lower than those found to other cell lines, such as SiHa and HeLa cells (IC_{50} = 42.2 ± 3.5 µM and 48.5 ± 4.2 µM, respectively) (Tsai et al., 2015) but identical to HN22 cells (IC_{50} = ~20 µM) (Cho et al., 2014). Blank NPs (PLGA NPs) up to 100 µg/mL (concentration equivalent to Lico-A; see methods) did not reduce cell viability (Fig. 2B) indicating the non-cytotoxic effect of these NPs. We also observed that the encapsulation of Lico-A reduces its toxicity (Fig. 2C-E) which is evident by the higher IC_{50} values and also by the higher concentration needed to significantly reduce cell viability comparing to control (red bars in each plot).

3.2.2. Anti-inflammatory effect of Lico-A and of NPs

The anti-inflammatory activity was assessed in LPS-stimulated RAW 264.7 cells (a macrophage cell line), as these cells when exposed to bacterial lipopolysaccharides (LPS) have the ability to release nitric oxide (NO) as a result of inflammatory signalling activated by LPS that culminates with enhancement of nitric oxide synthase activity. Thus, the

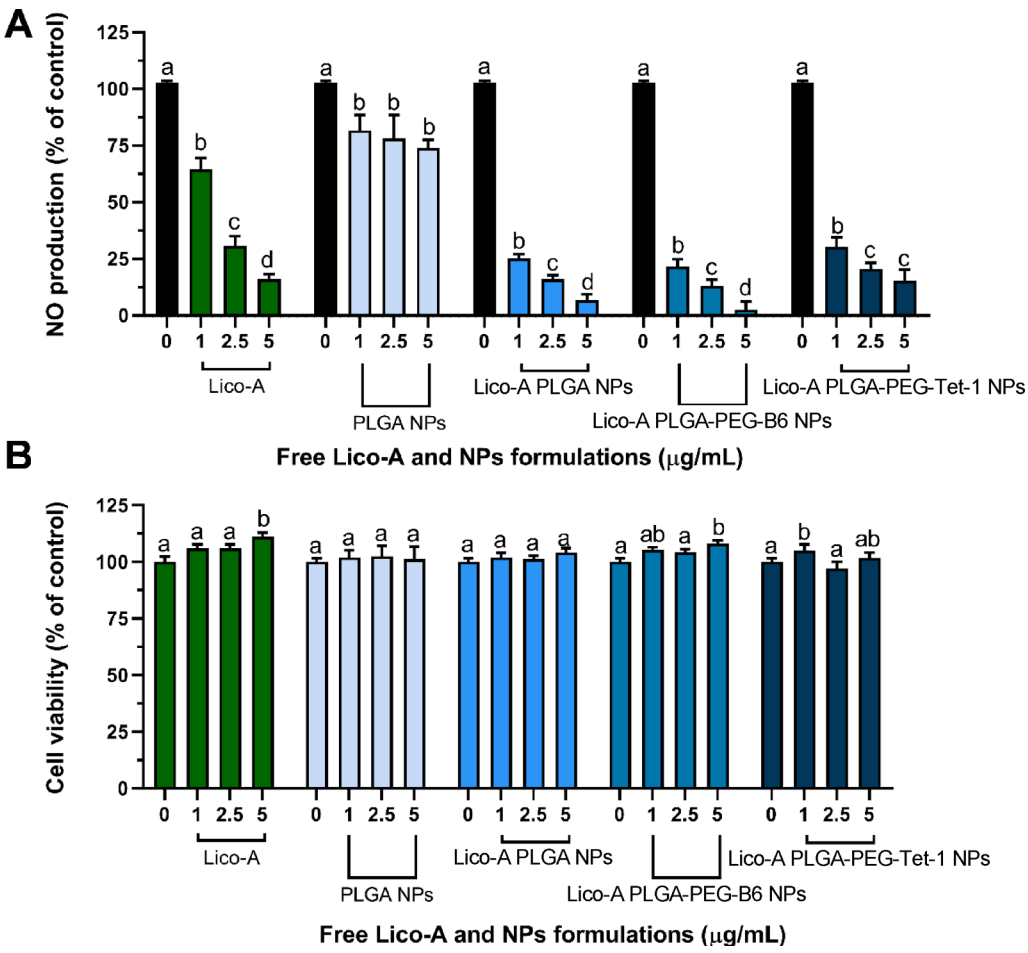

Fig. 3. Anti-inflammatory activity **(A)** and cell viability **(B)** of Lico-A, non-loaded NPs (PLGA NPS) and NPs formulations containing Lico-A (Lico-A PLGA NPs) and cell penetrating peptides B6 (Lico-A PLGA-PEG-B6 NPs) and Tet-1 (Lico-A PLGA-PEG-Tet-1 NPs) using the LPS-stimulated RAW 264.7 cell model. Anti-inflammatory activity was assessed by quantifying the NO released into the culture media (see methods), and cell viability was performed at the end of the assay (see methods for details). Results are expressed as mean ± SD (n = 4). Statistically significant differences ($p < 0.05$) between the control and sample concentrations are denoted with different letters within the same sample.

anti-inflammatory action of Lico-A and of four formulations was assessed by their ability to reduce the amount of NO released by LPS-stimulated macrophages, and results are shown in Fig. 3A. Lico-A has been reported as anti-inflammatory agent (Cai et al., 2023; Funakoshi-Tago et al., 2010; Galindo et al., 2022) and, indeed, it dose-dependently reduces NO release from LPS-stimulated macrophages. Raw 264–7 cells exposed for 4 h to 5 μg/mL of Lico-A only released ~ 16 % of NO compared to control (a NO reduction of ~ 84 % of control), denoting its action on TLR4 signalling pathways (Tun et al., 2018) and anti-inflammatory activity. At this concentration Lico-A was not cytotoxic to Raw 264–7 cells as cell viability assay indicates ~ 100 % cell viability (Fig. 3B). Blank NPs (PLGA NPs) *per se* reduce NO release, probably due to its lipid interference and potential competitive binding to TLR4 reducing the LPS activity; however, the action of NPs lipids on reduction of NO release needs further evaluation. Lico-A PLGA NPs show increased anti-inflammatory activity, compared to Lico-A in solution, probably due to improved delivery of Lico-A to the cells surface. Addition of cell penetrating peptides to Lico-A-PLGA NPs maintained the anti-inflammatory activity as shown in Fig. 3A (two rightmost panels). None of the formulations was toxic to RAW 264.7 cells, as cell viability is maintained at 100 % (Fig. 3B).

It is commonly reported that, when CPPs are administered alone, the cell viability is lower than the control; however, when linked to NPs, the toxicity is lower, increasing the biocompatibility of nanoparticles. This was the case of PC12 cells exposed to B6 peptide which showed a decrease in 35 % of viability compared to non-exposed cells (cell viability ~ 65 % of control), the same decrease was observed when exposed to SA-Se-NPs. However, and as reported by Yin et al. (2015) (Yin et al., 2015) when cells were treated with SA-Se-NPs conjugated with B6 peptide (B6-SA-Se-NPs) the cell viability was only reduced in 10 % from control. This means that functionalization of NPs with B6 resulted in lower toxicity, as happened in our work. In a study using curcumin as delivering molecule and B6 as CPP, Fan et al. (2018) (Fan et al., 2018) assessed the viability of HT22 cells exposed to different concentrations of curcumin (Cur), Cur-loaded PLGA-PEG, Cur-loaded PLGA-PEG-B6, and PLGA-PEG-B6. In this case, the authors observed no statistical differences between all samples, but cells exposed to Cur-loaded PLGA-PEG-B6 showed on average higher viability. This study also indicates that the functionalized particles were no more cytotoxic. In other study, published by Zhang et al. (2014) (Zhang et al., 2014), PC12 cells treated with EGCG-stabilized selenium nanoparticles coated with Tet-1 peptide (Tet-1-EGCG@Se) showed higher viability than cells exposed to EGCG@Se (selenium nanoparticles with EGCG attached onto the surface), also showing that the binding of CPPs to NPs does not increase cell toxicity. Conjugation of PLGA coated-curcumin nanoparticles with Tet-1, was also shown to result in biocompatible nanoparticles, without reporting higher toxicity against GI-1 glioma cells (Mathew et al., 2012).

In our study, we showed that encapsulation of LicoA reduces the inherent toxicity of the drug, attributed to the controlled drug release obtained when using nanoparticles. Besides, the functionalization of NPs with both CPPs improves biocompatibility (by reducing cell toxicity even more), as evidenced by the increase of the IC50. The aim of this work was the delivery of an anti-inflammatory drug while maintain cell viability. We show that encapsulation reduces the toxicity of LicoA and also improved the anti-inflammatory effect of LicoA. Also, conjugation of NPs with CPPs, namely with Tet-1, resulted in an increase of biocompatibility while with B6 it was equal to the NPs.

Table 2
Osmolality values of PLGA NPs nanoparticles in presence of different percentages of cryoprotectants.

Cryoprotectant % (w/v)		PLGA NPs Osmolality (mOsm/kg)	
		Without cryoprotectant	With cryoprotectant
Glycerol	0.5	282	324
	1	282	389
	3	286	416
Maltitol	0.5	286	288
	1	286	297
	3	286	303
Sucrose	0.5	284	300
	1	284	312
	3	285	324
Trehalose	0.5	285	294
	1	283	306
	3	283	337
Sorbitol	0.5	282	298
	1	282	303
	3	282	308

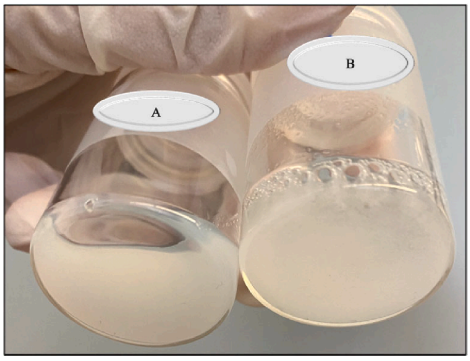

Fig. 4. Visual evaluation of PLGA NPs **(A)**; reconstituted sample of PLGA NPs with 3 % maltitol (w/v) **(B)**.

Table 3
Osmolality values of the optimized and functionalized NPs formulations in presence or not of the selected cryoprotectant at 3 % (w/v) and evaluation of the cake appearance after freeze-drying.

Formulations	Before freeze-drying Osmolality (mOsm/Kg)		After freeze-drying Cake appearance
	Without maltitol	With maltitol	
Lico-A PLGA NPs	295	307	Collapsed in the middle with raised edges. Rough and homogeneous cake, yellow in color and opaque.
	295	306	
Lico-A PLGA-PEG-B6 NPs	297	312	Thin film in the middle of vial height. Cake homogeneous, slightly porous, yellow in color and opaque.
	297	309	
Lico-A PLGA-PEG-Tet-1 NPs	298	317	Homogeneous, smooth, yellow in color, and opaque. Collapsed with shrinkage, flat, rough cake.
	298	312	

3.3. Freeze-drying

Glycerol, maltitol, sucrose, trehalose, and sorbitol were evaluated as possible cryoprotectants and were dissolved in PLGA NPs at 0.5, 1, and 3 % (w/v). In this phase, the osmolality was measured (Table 2) in order to assess the adequate range which should be similar to lacrimal fluid, around 302–318 mOsm/kg to avoid ocular irritation (Ramos Yacasi et al., 2017).

For the freeze-drying procedure was carried out according to the method described in section 2.5. Subsequently, the obtained cakes were reconstituted and compared in appearance with a fresh sample of blank NPs. The lyophilized pharmaceutical must retain the original product properties, low residual moisture, good cake appearance and fast reconstitution (Trenkenschuh and Friess, 2021).

Formulations with trehalose and maltitol at 3 % (w/v) obtained the shortest reconstitution times. On the other hand, sucrose freeze-dried nanoparticles at 0.5 % (w/v) took the longest time to reconstitute. In addition, maltitol samples showed the most similar visual appearance to the fresh samples of PLGA NPs (Fig. 4). Considering the values of osmolality, aspect of the dried cake, and the time and appearance of the reconstitutions, maltitol was chosen as the ideal cryoprotectant at the percentage of 3 % (w/v) for studies with Lico-A PLGA NPs, Lico-A PLGA-PEG-B6 NPs and Lico-A PLGA-PEG-Tet-1 NPs.

Once the cryoprotectant and its appropriate percentage were selected, the freeze-drying of the final formulations continued. Table 3 shows the results of the evaluation of Lico-A PLGA NPs and CPP-functionalized NPs. The osmolality values remained within the desired limits for formulations intended for ocular application and slight differences were found in the appearance of the cake after freeze-drying, possibly due to the structural difference from one CPP to another.

An important tool to predict the physical stability of freeze-dried products during storage is DSC analysis (Ataide et al., 2021). The cake obtained by freeze-dried nanoparticles must be stored at a temperature below the thermal transitions of the dried formulation to prevent any collapse, shrinkage or any other destabilization, such as crystallization to be pharmaceutically acceptable (Abdelwahed et al., 2006). Thermal profiles of freeze-dried formulations with maltitol at 3 % (w/v) were analyzed by DSC (Fig. 5) to check thermal transitions.

Thermogram of freeze-dried PLGA NPs with 3 % maltitol (w/v) (Fig. 5) showed a broad endothermic peak starting at about 94.2 °C with maximum at 111.2 °C, can be likely attributed to evaporation events. Volatilized residual moisture from freeze-dried products usually shows up in thermograms as broad endothermic peaks near the boiling point of water (Jones and Seyler, 1994). Moreover, the thermal analysis of all the freeze-dried formulations with this oligosaccharide-derived sugar alcohol, as expected according to the literature, presented a glass transition at above room temperature (Shirke et al., 2005). The glass transition temperature (T_g) was determined as the maximum inflection point of the discontinuities in the heat flow curves, being 57.2 °C to 66.4 °C with midpoint 62.1 °C for PLGA NPs; 39.6 °C to 46.1 °C with midpoint 43.4 °C for Lico-A PLGA NPs; 44.5 °C to 50.9 °C with midpoint 47.7 °C for Lico-A PLGA-PEG-B6 NPs and 48.4 °C to 50.8 °C with midpoint 49.1 °C for Lico-A PLGA-PEG-Tet-1 NPs. Higher T_g values of the formulations compared to the value of the cryoprotectant, could be due to the polymer since the presence of this excipient with high T_g is a way to raise the T_g of the amorphous sugar alcohol solid. In the case of the formulations of PLGA NPs and Lico-A-PLGA-Tet-1 NPs, endothermic peaks can be seen at 130.5 °C and 149.4 °C respectively, which might suggest partial crystallization of the freeze-drying process (Kadoya et al., 2010).

In the same way than the oligosaccharides, maltitol should substitute water molecules surrounding the NPs to maintain the conformation during the freeze-drying, due to its sufficient number of water-substituting hydrogen bonds, decreasing the magnitude of most physical and chemical changes that occur during storage (Kadoya et al., 2010).

3.4. In-situ forming gel formulation

The selection of the correct excipients is important for the purpose to achieve an optimal balance between ocular formulation properties and formulation effect on the ocular surface (Jurišić Dukovski et al., 2020). PF127 was used in the formulation to form an *in-situ* forming gel (ISFG). Regarding the concentration of PF127, systems composed of 20 % (w/w) FP127 exhibited mucoadhesive profile marginally higher than those containing 17.5 % (da Silva et al. (2021)). This polymer has the characteristic of allowing the formulation to remain liquid under storage conditions, but when it comes into contact with ocular temperature it

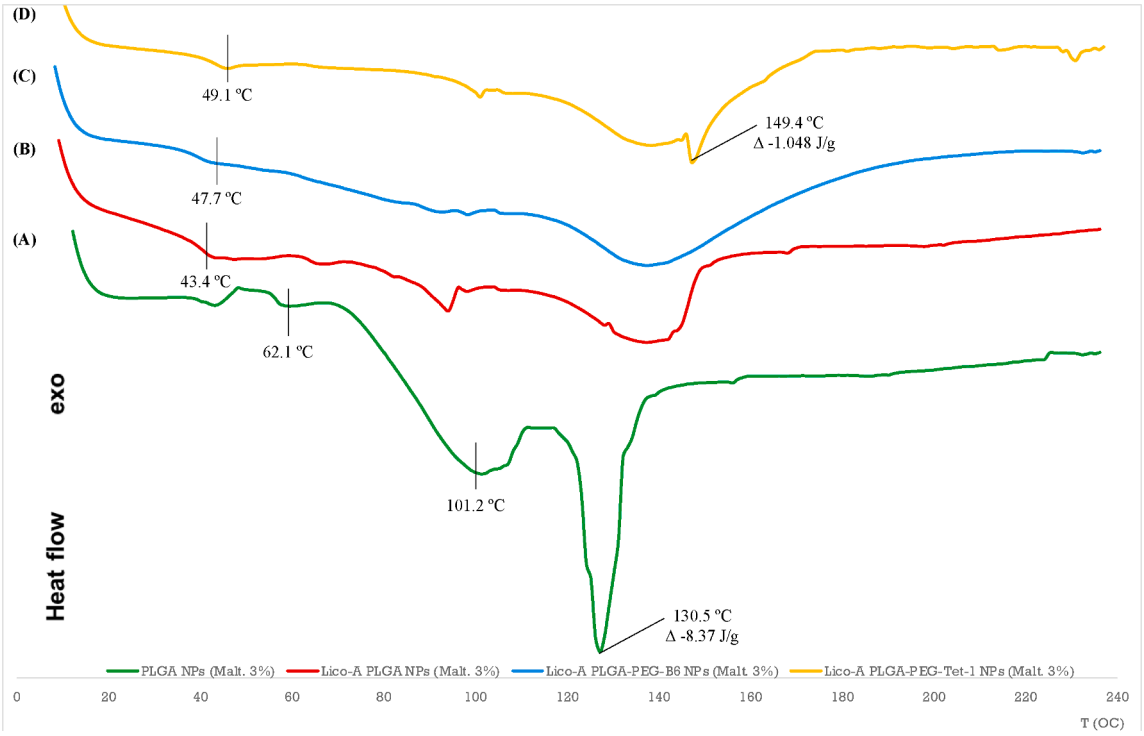

Fig. 5. DSC analysis after freeze-drying in presence of 3 % maltitol (w/v) of **(A)** PLGA NPs; **(B)** Lico-A PLGA NPs; **(C)** Lico-A PLGA-PEG-B6 NPs and **(D)** Lico-A PLGA-PEG-Tet-1 NPs.

Table 4
Composition and characterization of in-situ gel formulations.

Formulation	PF127 (w/v)	MC (w/v)	CTAB (w/v)	pH without buffer	pH with buffer	$T_{sol-gel}$ (°C)[a]
ISFG-1 PLGA NPs	20.0	0.0	0.2	6.94	7.39	37 ± 1.0
ISFG-2 PLGA NPs	20.0	0.5	0.2	6.91	7.36	32 ± 1.2
ISFG-3 PLGA NPs	20.0	1.0	0.2	6.97	7.42	22 ± 1.0
ISFG-1 Lico-A PLGA NPs	20.0	0.0	0.2	6.93	7.37	36 ± 0.6
ISFG-2 Lico-A PLGA NPs	20.0	0.5	0.2	6.83	7.38	32 ± 0.6
ISFG-3 Lico-A PLGA NPs	20.0	1.0	0.2	6.95	7.41	21 ± 1.2

[a] Mean (±SD) of at least three replicate measurements.

turns into a gel. With this peculiarity, precision was expected in the application of the formulation and that the contact time of the preparation in the precorneal area would be prolonged, reduce the elimination rate, and increasing the bioavailability of the drug (Cardoso et al., 2022). MC was used as a viscosity enhancing agent in different concentrations (that maintained the thermally reversible sol – gel characteristics of the PF127 based formulations) in an attempt not to use a higher concentration of PF127, and to obtain reasonable viscosity for the prepared formulations. An important and critical parameter for thermosensitive gel formulation is the gelation temperature ($T_{sol-gel}$). Since the average temperature of precorneal mucosa is ~ 35 °C (Tan et al., 2010), the optimal thermosensitive *in-situ* gel should have a $T_{sol-gel}$ above room temperature to ensure that the preparation remains liquid to provide accurate dosing (Krtalić et al., 2018), and the acceptable range of $T_{sol-gel}$ for thermosensitive *in-situ* ocular gel is 30–35 °C to avoid the rapid leakage out of the formulation (Permana et al., 2021). $T_{sol-gel}$ values of the formulations are shown in Table 4. ISFG-2 was selected as the optimal formulation.

The initial rheological test was performed with PLGA NPs and Lico-A PLGA NPs to select the optimal formulation. Three formulations of *in-situ* forming gel were tested ISFG-1, ISFG-2 and ISFG-3. The results of the viscosity illustrate that the increment of MC concentration increase the consistency of the gel, which corroborates the result obtained in the gelation temperature test. In aqueous systems, PF127 thermosensitive gels are formed by hydrogen bonding, due to the attraction between the poloxamer ether oxygen atom and the protons of water. Thus, by adding the MC amount (compound with hydroxyl groups), the number of hydrogen bonds is expected to increase, leading to higher viscosity (Mansour et al., 2008).

After that, a new rheological test was performed on the optimal formulation (ISFG-2) with PLGA NPs, Lico-A PLGA NPs, Lico-A PLGA-PEG-B6 NPs and Lico-A PLGA-PEG-Tet-1 NPs, with the aim of analyzing the viscosity which depend on temperature and shear rate, so the storage and application temperature of the formulation can be used as factors. In our study, formulations were tested at a controlled shear rate at two temperatures, 20 °C and 35 °C. The ocular temperature is approximately between 32 °C and 34 °C (Khattab et al., 2019), so this temperature corresponds to the application of *in-situ* forming gel on the pre-corneal area thus increasing its contact time with the ocular mucus membrane. The temperature of 20 °C correspond to the storage temperature, just before its application on the ocular surface. The impact of the different temperatures of the test on the consistency of the *in-situ* forming gel was shown in Fig. 6, where it was observed that the viscosity increased with the elevation of temperature. This could be explained, because a higher temperature caused the dehydration of the PEO/PPO/PEO triblock units of PF127 by the breakdown of the hydrogen bonds between PEO units and water. As a result, this dehydration leads to increasing the intermolecular interaction between PEO blocks and the copolymer molecules aggregate into micelles, allowing the formation of a more closely packed and a more viscous gel (El-Kamel, 2002; Kolsure and Rajkapoor, 2012).

The temperature and shear rate significantly affect the viscosity of the formulation. Fig. 6 shows the rheograms where the evolution of the

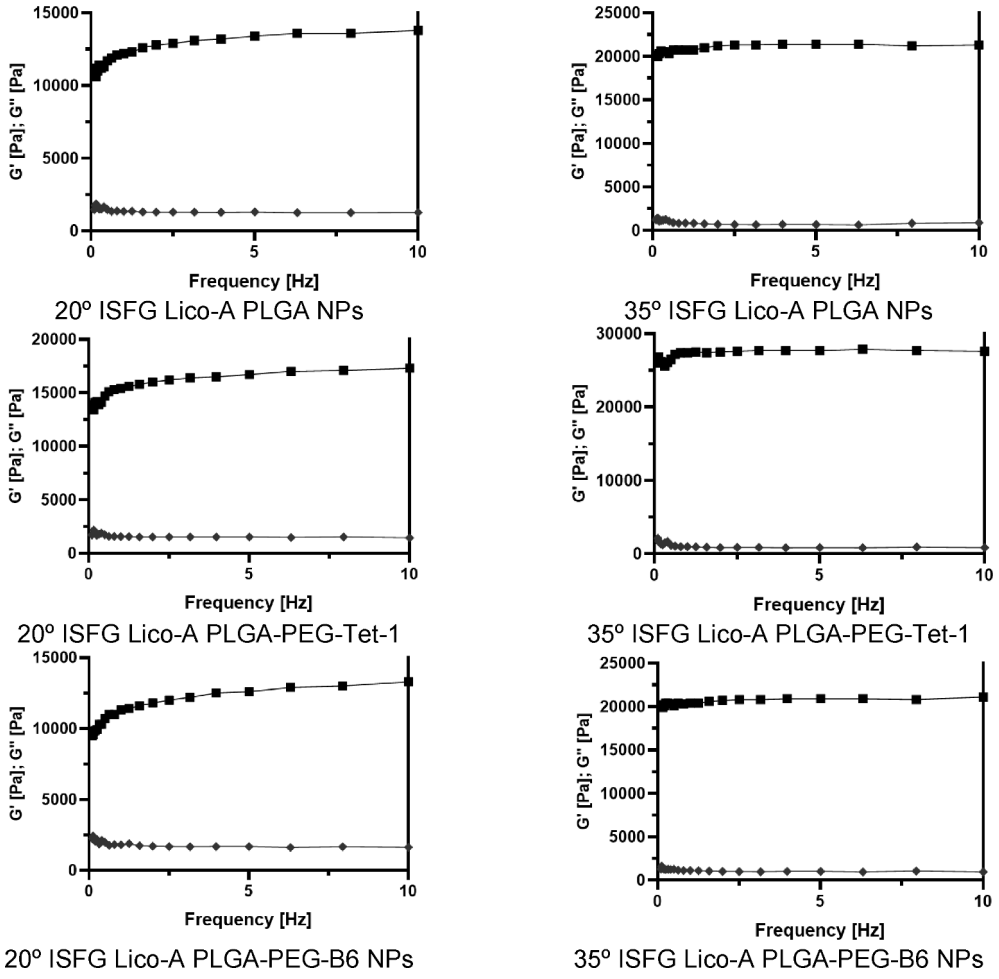

Fig. 6. Frequency-dependent changes in viscoelastic properties (■ storage modulus G' [Pa]; ▼loss modulus G" [Pa]) of the optimized in-situ forming gel with Lico-A PLGA NPs, Lico-A PLGA-PEG-Tet-1 NPs and Lico-A PLGA-PEG-B6 NPs at 20 °C and 35 °C.

Table 5
Texture profile analysis of the optimized in-situ forming gel with Lico-A-PLGA NPs, Lico-A PLGA-PEG-B6 NPs and Lico-A-PLGA-PEG-Tet-1 NPs.

Temperature	Parameter		ISFG Lico-A PLGA NPs	ISFG Lico-A PLGA-PEG-B6 NPs	ISFG Lico-A PLGA-PEG-Tet-1 NPs
20 °C	Hardness	Force (N)	0.055	0.058	0.056
		Gradient (N/sec)	0.001	0.001	0.001
	Firmness	Force (N)	31.714	26.426	26.468
		Separation (mm)	0.165	0.15	0.375
	Mucoadhesiveness	Negative force (N)	−29.328	−26.331	−23.228
		Gradient (g/sec)	5.268	4.167	4.215
	Spreadability	Force (N)	2.73	2.983	1.803
		Separation (mm)	3.738	5.048	3.688
35 °C	Hardness	Force (N)	29.289	28.815	28.592
		Gradient (N/sec)	9.624	9.476	9.395
	Firmness	Force (N)	98.448	98.153	107.324
		Separation (mm)	0.06	0.045	0.075
	Mucoadhesiveness	Negative force (N)	−81.393	−84.939	−73.931
		Gradient (g/sec)	18.627	18.512	20.299
	Spreadability	Force (N)	10.628	10.261	11.871
		Separation (mm)	9.9	12.15	10.85

dynamic modules with respect to frequency is observed. It is clear that the results revealing suitable gel stability and a viscoelastic gel behavior. In all the formulations there is no crossover point between the modules, behaving like a weak-gel (de Castro et al., 2022; Krtalić et al., 2018). The rheograms obtained during tests at two temperatures, 20 °C and 35 °C, show slight changes of the shape of the overall rheogram as the temperature increases. At 35 °C, an increase in the distance between the modules G' and G" was observed for each formulation, which is the result of higher shear stress due to the increase in viscosity at this temperature. Regarding the point of view of the ocular application of the *in-situ* gel, it is a beneficial phenomenon to increase the contact of the formulation with the pre-corneal mucosa because the temperature of 35 °C corresponds to the temperature on the ocular surface. After administration, the formulation is expected to form a gel (G'> G") and, in this way, withstands the shearing forces expected in the eye during and between blinking (Cardoso et al., 2022). These results indicated that

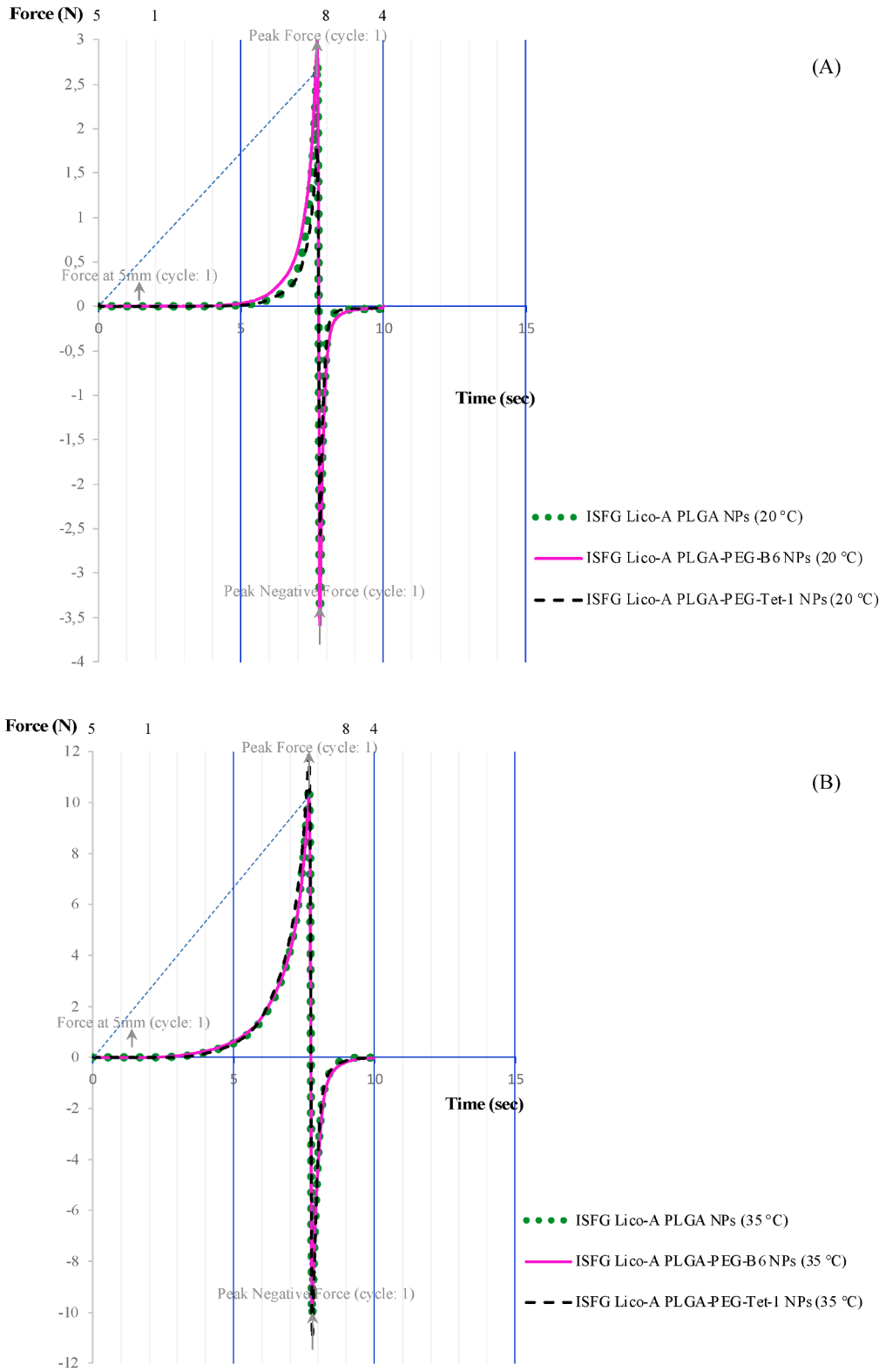

Fig. 7. Spreadability performance of the optimized in-situ forming gel loaded Lico-A PLGA NPs, Lico-A PLGA-PEG-B6 NPs and Lico-A PLGA-PEG-Tet-1 NPs at **(A)** 20 °C and **(B)** 35 °C.

the formulations containing CPPs can increase the viscosity as the temperature increases, but the $T_{sol\text{-}gel}$ does not occur until 32 °C.

Texture analysis provides instrumental information on some structure properties of products and can predict the characteristics of the formulation *in vivo* (De Souza Ferreira et al., 2017). Results of texture analysis are important for the development of topical dosage forms because the patient acceptability of the product depends mostly on its application and organoleptic attributes. The analysis of texture parameters, hardness, firmness, mucoadhesiveness and spreadability are directly influenced by the viscosity of the formulations. Textural properties are displayed in Table 5. The measurement of mechanical characteristics such as hardness and firmness for *in-situ* forming gel, could be

calculated from the plotted of force versus distance, these parameters are very important, and the results presented in Table 5. To facilitate application at the time of use, the formulation must have adequate strength, must be lower enough to ensure the easy administration but not too low to avoid rapid drainage of the formulation from the eye, and not too stiff to prevent patient discomfort (Khattab et al., 2019). Hardness is the force required to attain a given deformation of the gel and is a measure of the easiness of application of the gel at the site of action. Gel strength provides evidence about the firmness of the gelled structure and it is directly proportional to hardness, firmness provides the capability of the gel to resist the mucociliary clearance in the target area (Dawre et al., 2022). Thus, as shown in Table 5, At 20 °C, the temperature during administration, all formulation were is semi-liquid form and showed low values of hardness and firmness, these low values facilitate the correct withdrawal of the product from the container (Said dos Santos et al., 2020). The increase in analysis temperature from 20 °C to 35 °C, was followed by an increase of hardness and firmness of *in-situ* forming gels. These findings are due to the modifications in the internal structure of the poloxamer, exhibiting a stronger polymeric network (El-Kamel, 2002; Kolsure and Rajkapoor, 2012). For example, in the case of ISFG loaded Lico-A PLGA NPs, Lico-A PLGA-PEG-B6 NPs and Lico-A PLGA-PEG-Tet-1 NPs at 35 °C the hardness was much higher in comparison with the analysis at 20 °C for the same formulations, presenting values from 29.3 N, 28.8 N and 28.6 N respectively, and firmness in the same way for the ISFG loaded NPs. Increasing the temperature from 20 °C to 35 °C led to increasing the hardness and firmness, indicating an adequate gel consistency to keep the formulation with no deformation at the site of action (Jones et al., 1997). The influence of hardness on the retention time of the formulation on the target site has been studied, since the adequate hardness prevents the preparation dilution by mucociliary clearance (De Souza Ferreira et al., 2017).

Formulations that have been designed for topical use in the eye must show adhesion to mucosal surface as this will decrease their clearance time, and thus improve clinical efficacy. Adhesiveness is defined as the work required to overcome the attractive forces between the surface of the sample and the surface of the probe (Pandey et al., 2017). With mucoadhesive studies performed at/near the target ocular temperature (35 °C) the highest value of mucoadhesion was found with ISFG Lico-A PLGA-PEG-B6 NPs where recorded a negative force of –84.9 N. As we expected the lowest value of work was shown by ISFG loaded NPs at 20 °C. These results showed that as temperature of test was increased, a concomitant increase in mucoadhesion was observed and this is explained by the viscosity impact on this parameter during the analysis. Our studies revealed that ISFG Lico-A PLGA-PEG-Tet-1 NPs displayed the lowest mucoadhesion/adhesiveness between formulation and the probe; this can be attributed to its relatively different structure. Regarding the adhesion strength, it increased with increasing temperature, due to FP127 organization by $T_{sol\text{-}gel}$. As a result, the higher adhesiveness values at 35 °C from *in-situ* forming gel formulations is a desirable result, because it means, they can adhere to the application surface for a sufficiently long time, which may affect the druǵs residence time at the application site (Andrews et al., 2009; Pandey et al., 2017). In line with earlier reports indicating good mucoadhesive properties of a formula combination of PF127 and MC (Soliman et al., 2019).

On the other hand, it could be expected that the increases of the temperature would increase in the gel viscosity and thus decrease its spreadability. In this case, a suitable spreadability value, facilitates its spreading to a large surface area of ocular mucosa. At 20 °C we obtained high values of spreadability (less force is required). For instance, ISFG loaded Lico-A PLGA-PEG-B6 NPs at 35 °C seems to be the better spreadability results, in comparison with the other formulations at the same evaluation temperature. The spreadability plot in Fig. 7 illustrates the test results at storage and application temperatures. All these properties may be useful in expecting the formula behavior in different environmental and biological conditions.

4. Conclusions

In this study, Lico-A PLGA NPs functionalized with CPPs (B6 and Tet-1) were produced by solvent displacement method with adequate average size, polydispersity index, zeta potential and encapsulation efficiency. Results of *in vitro* biological experiments in Caco-2 and RAW 264.7 cell lines, showed a relevant anti-inflammatory activity and non-cytotoxic effect. Furthermore, the stability of the nanoparticles, was improved by freeze-drying and encapsulation in a thermosensitive hydrogel. In this sense, Lico-A PLGA NPs functionalized with CPPs were freeze-dried in the presence of different cryoprotectants, and the redispersibility of NPs in the reconstituted suspension was then evaluated to compare the osmolality, the time and appearance of the reconstitutions and the anti-aggregation effect of the different additives. The appearance of the freeze-dried cakes with 3 % maltitol (w/v) and their reconstituted nanosuspensions, revealed a fast reconstitution time, and full redispersion of NPs with no apparent aggregates. On the other hand, PF127 (20 % w/v) was used to prepare a thermosensitive *in-situ* forming gel with Lico-A PLGA NPs functionalized with CPPs for ocular administration. The formulation was maintained in a flowing semi-liquid state under non-physiological conditions and transformed into a semi-solid state under ocular temperature conditions (35 °C), which is beneficial for ocular administration. The pH, viscosity, texture parameters and gelation temperature results met the requirements for ophthalmic formulations. The gel has characteristics of viscoelasticity, suitable mechanical and mucoadhesive performance which facilitate its uniform distribution over the conjunctiva surface. Unlike eye drops, gels prolong ocular retention time, reducing the frequency of administration and improving patienťs compliance. For all the above, these appropriately formulated thermosensitive *in-situ* forming gels offer an alternative solution to current challenges in ocular drug delivery. This is of great clinical significance regarding the use of Licochalcone-A for treating ocular inflammations and provide a new pharmaceutical form for nanoparticles functionalized with CPPs.

Declaration of Competing Interest

The authors declare that they have no known competing financial interests or personal relationships that could have appeared to influence the work reported in this paper.

Data availability

Data will be made available on request.

Acknowledgements

R. M. Galindo-Camacho acknowledges the financial support of the Generalitat de Catalunya for the PhD scholarship FI-DGR EMC/2199/2017 (DOGC-7459-2017) and for the scholarship Santander Research/Convocatòria d'estades 2022 per a doctorands de la UB. Author are also thankful to the Spanish Ministry of Economy, Industry and Competitiveness, and the European Regional Development Fund (grants RTI2018-094120-B-I00 and PID2021-122216OB-I00). E. B. Souto wishes to acknowledge the national funds from FCT—Fundação para a Ciência e a Tecnologia, I.P., in the scope of the project UIDP/04378/2020 and UIDB/04378/2020 of the Research Unit on Applied Molecular Biosciences—UCIBIO and the project LA/P/0140/2020 of the Associate Laboratory Institute for Health and Bioeconomy—i4HB

References

Abdelwahed, W., Degobert, G., Stainmesse, S., Fessi, H., 2006. Freeze-drying of nanoparticles: Formulation, process and storage considerations. Adv. Drug Deliv. Rev. 58, 1688–1713.

Ali, Y., Lehmussaari, K., 2006. Industrial perspective in ocular drug delivery. Adv. Drug Deliv. Rev. 58, 1258–1268.

Andreani, T., Kiill, C.P., de Souza, A.L.R., Fangueiro, J.F., Fernandes, L., Doktorovova, S., Santos, D.L., Garcia, M.L., Gremiao, M.P.D., Souto, E.B., Silva, A.M., 2014. Surface engineering of silica nanoparticles for oral insulin delivery: Characterization and cell toxicity studies. Colloid Surface B 123, 916–923.
Andrews, G.P., Laverty, T.P., Jones, D.S., 2009. Mucoadhesive polymeric platforms for controlled drug delivery. Eur. J. Pharm. Biopharm. 71, 505–518.
Ataide, J.A., Geraldes, D.C., Gérios, E.F., Bissaco, F.M., Cefali, L.C., Oliveira-Nascimento, L., Mazzola, P.G., 2021. Freeze-dried chitosan nanoparticles to stabilize and deliver bromelain. J. Drug Delivery Sci. Technol. 61, 102225.
Badran, M.M., Alomrani, A.H., Harisa, G.I., Ashour, A.E., Kumar, A., Yassin, A.E., 2018. Novel docetaxel chitosan-coated PLGA/PCL nanoparticles with magnified cytotoxicity and bioavailability. Biomed. Pharmacother. 106, 1461–1468.
Bai, L., Lei, F., Luo, R., Fei, Q., Zheng, Z., He, N., Gui, S., 2022. Development of a Thermosensitive In-Situ Gel Formulations of Vancomycin Hydrochloride: Design, Preparation, In Vitro and In Vivo Evaluation. J. Pharm. Sci. 111, 2552–2561.
Cai, M., Xu, Y.-C., Deng, B., Chen, J.-B., Chen, T.-F., Zeng, K.-F., Chen, S., Deng, S.-H., Tan, Z.-B., Ding, W.-J., Zhang, S.-W., Liu, B., Zhang, J.-Z., 2023. Radix Glycyrrhizae extract and licochalcone a exert an anti-inflammatory action by direct suppression of toll like receptor 4. J. Ethnopharmacol. 302, 115869.
Carbone, C., Martins-Gomes, C., Caddeo, C., Silva, A.M., Musumeci, T., Pignatello, R., Puglisi, G., Souto, E.B., 2018. Mediterranean essential oils as precious matrix components and active ingredients of lipid nanoparticles. Int. J. Pharm. 548, 217–226.
Cardoso, C.O., Ferreira-Nunes, R., Cunha-Filho, M., Gratieri, T., Gelfuso, G.M., 2022. In situ gelling microemulsion for topical ocular delivery of moxifloxacin and betamethasone. J. Mol. Liq. 360, 119559.
Cho, J.J., Chae, J.-I., Yoon, G., Kim, K.H., Cho, J.H., Cho, S.-S., Cho, Y.S., Shim, J.-H., 2014. Licochalcone A, a natural chalconoid isolated from Glycyrrhiza inflata root, induces apoptosis via Sp1 and Sp1 regulatory proteins in oral squamous cell carcinoma. Int. J. Oncol. 45, 667–674.
Comstock, T.L., DeCory, H.H., 2012. Advances in Corticosteroid Therapy for Ocular Inflammation: Loteprednol Etabonate. Int. J. Inflamm. 2012, 789623.
da Silva, J.B., dos Santos, R.S., da Silva, M.B., Braga, G., Cook, M.T., Bruschi, M.L., 2021. Interaction between mucoadhesive cellulose derivatives and Pluronic F127: Investigation on the micelle structure and mucoadhesive performance. Mater. Sci. Eng. C 119, 111643.
Dawre, S., Waghela, S., Saraogi, G., 2022. Statistically designed vitamin D3 Encapsulated PLGA microspheres dispersed in thermoresponsive in-situ gel for nasal delivery. J. Drug Delivery Sci. Technol. 75, 103688.
de Castro, K.C., Côco, J.C., dos Santos, É.M., Ataide, J.A., Martinez, R.M., do Nascimento, M.H.M., Prata, J., da Fonte, P.R.M.L., Severino, P., Mazzola, P.G., Baby, A.R., Souto, E.B., de Araujo, D.R., Lopes, A.M., 2022. Pluronic® triblock copolymer-based nanoformulations for cancer therapy: a 10-year overview. Journal of Controlled Release (revised).
De Souza Ferreira, S.B., Da Silva, J.B., Borghi-Pangoni, F.B., Junqueira, M.V., Bruschi, M. L., 2017. Linear correlation between rheological, mechanical and mucoadhesive properties of polycarbophil polymer blends for biomedical applications. J. Mech. Behav. Biomed. Mater. 68, 265–275.
El-Haddad, M.E., Hussien, A.A., Saeed, H.M., Farid, R.M., 2021. Down regulation of inflammatory cytokines by the bioactive resveratrol-loaded chitoniosomes in induced ocular inflammation model. J. Drug Delivery Sci. Technol. 66, 102787.
El-Kamel, A.H., 2002. In vitro and in vivo evaluation of Pluronic F127-based ocular delivery system for timolol maleate. Int. J. Pharm. 241, 47–55.
Fan, S., Zheng, Y., Liu, X., Fang, W., Chen, X., Liao, W., Jing, X., Lei, M., Tao, E., Ma, Q., Zhang, X., Guo, R., Liu, J., 2018. Curcumin-loaded PLGA-PEG nanoparticles conjugated with B6 peptide for potential use in Alzheimer's disease. Drug Deliv. 25, 1091–1102.
Funakoshi-Tago, M., Nakamura, K., Tsuruya, R., Hatanaka, M., Mashino, T., Sonoda, Y., Kasahara, T., 2010. The fixed structure of Licochalcone A by α, β-unsaturated ketone is necessary for anti-inflammatory activity through the inhibition of NF-κB activation. Int. Immunopharmacol. 10, 562–571.
Galindo, R., Sánchez-López, E., Gómara, M.J., Espina, M., Ettcheto, M., Cano, A., Haro, I., Camins, A., García, M.L., 2022. Development of Peptide Targeted PLGA-PEGylated Nanoparticles Loading Licochalcone-A for Ocular Inflammation. Pharmaceutics 14, 285.
Gause, S., Hsu, K.-H., Shafor, C., Dixon, P., Powell, K.C., Chauhan, A., 2016. Mechanistic modeling of ophthalmic drug delivery to the anterior chamber by eye drops and contact lenses. Adv. Colloid Interface Sci. 233, 139–154.
Gessner, I., Neundorf, I., 2020. Nanoparticles Modified with Cell-Penetrating Peptides: Conjugation Mechanisms, Physicochemical Properties, and Application in Cancer Diagnosis and Therapy. Int. J. Mol. Sci. 21.
Gonzalez-Pizarro, R., Carvajal-Vidal, P., Halbault Bellowa, L., Calpena, A.C., Espina, M., García, M.L., 2019. In-situ forming gels containing fluorometholone-loaded polymeric nanoparticles for ocular inflammatory conditions. Colloids Surf. B Biointerfaces 175, 365–374.
Guo, W., Liu, B., Yin, Y., Kan, X., Gong, Q., Li, Y., Cao, Y., Wang, J., Xu, D., Ma, H., Fu, S., Liu, J., 2019. Licochalcone A Protects the Blood-Milk Barrier Integrity and Relieves the Inflammatory Response in LPS-Induced Mastitis. Front. Immunol. 10.
Jones, K., Seyler, R., 1994. Differential scanning calorimetry for boiling points and vapor pressure. NATAS Notes 26, 61–69.
Jones, D.S., Woolfson, A.D., Brown, A.F., 1997. Textural, viscoelastic and mucoadhesive properties of pharmaceutical gels composed of cellulose polymers. Int. J. Pharm. 151, 223–233.
Jurišić Dukovski, B., Juretić, M., Bračko, D., Randjelović, D., Savić, S., Crespo Moral, M., Diebold, Y., Filipović-Grčić, J., Pepić, I., Lovrić, J., 2020. Functional ibuprofen-loaded cationic nanoemulsion: Development and optimization for dry eye disease treatment. Int. J. Pharm. 576, 118979.
Kadowaki, M., Matsuura, T., Imanaka, H., Ishida, N., Imamura, K., 2022. Extraordinary high preservation of the dispersion state of Au nanoparticles during freeze-thawing and freeze-drying with gum arabic. Colloids Surf. A Physicochem. Eng. Asp. 639, 128392.
Kadoya, S., Fujii, K., Izutsu, K., Yonemochi, E., Terada, K., Yomota, C., Kawanishi, T., 2010. Freeze-drying of proteins with glass-forming oligosaccharide-derived sugar alcohols. Int. J. Pharm. 389, 107–113.
Khattab, A., Marzok, S., Ibrahim, M., 2019. Development of optimized mucoadhesive thermosensitive pluronic based in situ gel for controlled delivery of Latanoprost: Antiglaucoma efficacy and stability approaches. J. Drug Delivery Sci. Technol. 53, 101134.
Kolsure, P.K., Rajkapoor, B., 2012. Development of zolmitriptan gel for nasal administration. Asian J. Pharm. Clin. Res. 5, 88–94.
Krtalić, I., Radošević, S., Hafner, A., Grassi, M., Nenadić, M., Cetina-Čižmek, B., Filipović-Grčić, J., Pepić, I., Lovrić, J., 2018. D-Optimal Design in the Development of Rheologically Improved In Situ Forming Ophthalmic Gel. J. Pharm. Sci. 107, 1562–1571.
Kulkarni, S.S., Suryanarayanan, R., Rinella, J.V., Bogner, R.H., 2018. Mechanisms by which crystalline mannitol improves the reconstitution time of high concentration lyophilized protein formulations. Eur. J. Pharm. Biopharm. 131, 70–81.
Liu, X., Xing, Y., Li, M., Zhang, Z., Wang, J., Ri, M., Jin, C., Xu, G., Piao, L., Jin, H., Zuo, H., Ma, J., Jin, X., 2021. Licochalcone A inhibits proliferation and promotes apoptosis of colon cancer cell by targeting programmed cell death-ligand 1 via the NF-κB and Ras/Raf/MEK pathways. J. Ethnopharmacol. 273, 113989.
Luo, W.-C., O'Reilly Beringhs, A., Kim, R., Zhang, W., Patel, S.M., Bogner, R.H., Lu, X., 2021. Impact of formulation on the quality and stability of freeze-dried nanoparticles. Eur. J. Pharm. Biopharm. 169, 256–267.
Mahboobian, M.M., Mohammadi, M., Mansouri, Z., 2020. Development of thermosensitive in situ gel nanoemulsions for ocular delivery of acyclovir. J. Drug Delivery Sci. Technol. 55, 101400.
Makadia, H.K., Siegel, S.J., 2011. Poly Lactic-co-Glycolic Acid (PLGA) as Biodegradable Controlled Drug Delivery Carrier. Polymers 3, 1377–1397.
Mansour, M., Mansour, S., Mortada, N.D., Abd ElHady, S.S., 2008. Ocular Poloxamer-Based Ciprofloxacin Hydrochloride In Situ Forming Gels. Drug Dev. Ind. Pharm. 34, 744–752.
Mathew, A., Fukuda, T., Nagaoka, Y., Hasumura, T., Morimoto, H., Yoshida, Y., Maekawa, T., Venugopal, K., Kumar, D.S., 2012. Curcumin Loaded-PLGA Nanoparticles Conjugated with Tet-1 Peptide for Potential Use in Alzheimer's Disease. PLoS One 7, e32616.
Maulvi, F.A., Shetty, K.H., Desai, D.T., Shah, D.O., Willcox, M.D.P., 2021. Recent advances in ophthalmic preparations: Ocular barriers, dosage forms and routes of administration. Int. J. Pharm. 608, 121105.
Mazet, R., Yaméogo, J.B.G., Wouessidjewe, D., Choisnard, L., Gèze, A., 2020. Recent Advances in the Design of Topical Ophthalmic Delivery Systems in the Treatment of Ocular Surface Inflammation and Their Biopharmaceutical Evaluation. Pharmaceutics 12.
Mittal, A., Kakkar, R., 2021. Synthetic methods and biological applications of retrochalcones isolated from the root of Glycyrrhiza species: A review. Results Chem. 3, 100216.
Mobaraki, M., Soltani, M., Zare Harofte, S., E, L.Z., Daliri, R., Aghamirsalim, M., Raahemifar, K., 2020. Biodegradable Nanoparticle for Cornea Drug Delivery: Focus Review. Pharmaceutics 12.
Mohd Shahrizan, M.S., Abd Aziz, Z.H., Katas, H., 2022. Fluid gels: A systematic review towards their application in pharmaceutical dosage forms and drug delivery systems. J. Drug Delivery Sci. Technol. 67, 102947.
Oliveira, N., Cádiz-Gurrea, M.d.l.L., Silva, A.M., Macedo, C., Rodrigues, F., Costa, P., 2022. Development and Optimization of a Topical Formulation with Castanea sativa Shells Extract Based on the Concept “Quality by Design&rdquo. Sustainability 14, 129.
Pandey, P., Cabot, P.J., Wallwork, B., Panizza, B.J., Parekh, H.S., 2017. Formulation, functional evaluation and ex vivo performance of thermoresponsive soluble gels - A platform for therapeutic delivery to mucosal sinus tissue. Eur. J. Pharm. Sci. 96, 499–507.
Permana, A.D., Utami, R.N., Layadi, P., Himawan, A., Juniarti, N., Anjani, Q.K., Utomo, E., Mardikasari, S.A., Arjuna, A., Donnelly, R.F., 2021. Thermosensitive and mucoadhesive in situ ocular gel for effective local delivery and antifungal activity of itraconazole nanocrystal in the treatment of fungal keratitis. Int. J. Pharm. 602, 120623.
Ramos Yacasi, G.R., Calpena Campmany, A.C., Egea Gras, M.A., Espina García, M., García López, M.L., 2017. Freeze drying optimization of polymeric nanoparticles for ocular flurbiprofen delivery: effect of protectant agents and critical process parameters on long-term stability. Drug Dev. Ind. Pharm. 43, 637–651.
Said dos Santos, R., Rosseto, H.C., Bassi da Silva, J., Vecchi, C.F., Caetano, W., Bruschi, M.L., 2020. The effect of carbomer 934P and different vegetable oils on physical stability, mechanical and rheological properties of emulsion-based systems containing propolis. J. Mol. Liq. 307, 112969.
Severino, P., Andreani, T., Jager, A., Chaud, M.V., Santana, M.H.A., Silva, A.M., Souto, E. B., 2014. Solid lipid nanoparticles for hydrophilic biotech drugs: Optimization and cell viability studies (Caco-2 & HEPG-2 cell lines). Eur. J. Med. Chem. 81, 28–34.
Shirke, S., Takhistov, P., Ludescher, R.D., 2005. Molecular Mobility in Amorphous Maltose and Maltitol from Phosphorescence of Erythrosin B. J. Phys. Chem. B 109, 16119–16126.
Silva, A.M., Martins-Gomes, C., Fangueiro, J.F., Andreani, T., Souto, E.B., 2019. Comparison of antiproliferative effect of epigallocatechin gallate when loaded into

cationic solid lipid nanoparticles against different cell lines. Pharm. Dev. Technol. 24, 1243–1249.
Silva, A.M., Martins-Gomes, C., Souto, E.B., Schäfer, J., Santos, J.A., Bunzel, M., Nunes, F.M., 2020. Thymus zygis subsp. zygis an Endemic Portuguese Plant: Phytochemical Profiling, Antioxidant, Anti-Proliferative and Anti-Inflammatory Activities. Antioxidants 9, 482.
Silva, A.M., Félix, L.M., Teixeira, I., Martins-Gomes, C., Schäfer, J., Souto, E.B., Santos, D. J., Bunzel, M., Nunes, F.M., 2021. Orange thyme: Phytochemical profiling, in vitro bioactivities of extracts and potential health benefits. Food Chemistry: X 12, 100171.
Singla, P., Garg, S., McClements, J., Jamieson, O., Peeters, M., Mahajan, R.K., 2022. Advances in the therapeutic delivery and applications of functionalized Pluronics: A critical review. Adv. Colloid Interface Sci. 299, 102563.
Soliman, K.A., Ullah, K., Shah, A., Jones, D.S., Singh, T.R.R., 2019. Poloxamer-based in situ gelling thermoresponsive systems for ocular drug delivery applications. Drug Discov. Today 24, 1575–1586.
Sylvester, B., Porfire, A., Achim, M., Rus, L., Tomuță, I., 2018. A step forward towards the development of stable freeze-dried liposomes: a quality by design approach (QbD). Drug Dev. Ind. Pharm. 44, 385–397.
Tan, J.-H., Ng, E.Y.K., Rajendra Acharya, U., Chee, C., 2010. Study of normal ocular thermogram using textural parameters. Infrared Phys. Technol. 53, 120–126.
Trenkenschuh, E., Friess, W., 2021. Freeze-drying of nanoparticles: How to overcome colloidal instability by formulation and process optimization. Eur. J. Pharm. Biopharm. 165, 345–360.
Tsai, J.-P., Lee, C.-H., Ying, T.-H., Lin, C.-L., Lin, C.-L., Hsueh, J.-T., Hsieh, Y.-H., 2015. Licochalcone A induces autophagy through PI3K/Akt/mTOR inactivation and autophagy suppression enhances Licochalcone A-induced apoptosis of human cervical cancer cells. Oncotarget 6.
Tun, X., Yasukawa, K., Yamada, K.-I., 2018. Nitric Oxide Is Involved in Activation of Toll-Like Receptor 4 Signaling through Tyrosine Nitration of Src Homology Protein Tyrosine Phosphatase 2 in Murine Dextran Sulfate-Induced Colitis. Biol. Pharm. Bull. 41, 1843–1852.
Wang, Z., Xue, Y., Chen, T., Du, Q., Zhu, Z., Wang, Y., Wu, Y., Zeng, Q., Shen, C., Jiang, C., Yang, Z., Zhu, H., Liu, L., Liu, Q., 2021. Glycyrrhiza acid micelles loaded with licochalcone A for topical delivery: Co-penetration and anti-melanogenic effect. Eur. J. Pharm. Sci. 167, 106029.
Wang, Z., Xue, Y., Zeng, Q., Zhu, Z., Wang, Y., Wu, Y., Shen, C., Zhu, H., Jiang, C., Liu, L., Liu, Q., 2022. Glycyrrhiza acid-Licochalcone A complexes for enhanced bioavailability and anti-melanogenic effect of Licochalcone A: cellular uptake and in vitro experiments. J. Drug Delivery Sci. Technol. 68, 103037.
Yin, T., Yang, L., Liu, Y., Zhou, X., Sun, J., Liu, J., 2015. Sialic acid (SA)-modified selenium nanoparticles coated with a high blood–brain barrier permeability peptide-B6 peptide for potential use in Alzheimer's disease. Acta Biomater. 25, 172–183.
Yun, Y.H., Lee, B.K., Park, K., 2015. Controlled Drug Delivery: Historical perspective for the next generation. J. Control Release 219, 2–7.
Zhang, J., Zhou, X., Yu, Q., Yang, L., Sun, D., Zhou, Y., Liu, J., 2014. Epigallocatechin-3-gallate (EGCG)-Stabilized Selenium Nanoparticles Coated with Tet-1 Peptide To Reduce Amyloid-β Aggregation and Cytotoxicity. ACS Appl. Mater. Interfaces 6, 8475–8487.